

Ozren Husnjak
Veski Ltd
ozren.husnjak@veski.hr

John Letal
Qualitrol (Iris Power)
jletal@qualitrolcorp.com

Ozren Orešković
Veski Ltd
ozren.oreskovic@veski.hr

Fabian Kaica
Fabian Kaica Consulting, Australia
fabiankaica@netspace.net.au

Dynamical loads and the consequences in the Rough Load Zone Operation – case studies

SUMMARY

Hydro units powered by Francis turbines often experience operational zones with significant hydrodynamical and mechanical instabilities. These zones are referred to as the Rough Load Zones (RLZ). Typically, the instabilities occur at 30-50% loads, but under certain conditions they can also be present up to 70% of nominal load.

In the RLZ vortices form in the draft tube below the turbine due to the pressure pulsations forming below the turbine runner. This can lead to large rotor vibrational response, related to operation in the RLZ in the turbine region and in the thrust (axial) bearing region as well. The direct consequences of RLZ operation are often large axial loads which can be measured on the axial (thrust) bearing bracket and generally increased vibration levels in axial and radial directions.

One example of very prominent dynamical instabilities is on a 120 MW, 120 RPM unit where the RLZ extends from ~30 to ~80 MW (25 to 67%). The vibrational response in the axial direction is so large that the rotor vibrational displacements exceeded 2 mm peak-to-peak ($v_{RMS} = 1.3$ mm/s). This poses a direct threat to the thrust bearing structure and the supporting concrete foundations. Therefore, cracks were found in the axial bearing foundations on this plant. An experimental identification procedure was performed, and suggestions provided to reduce the vibrational response in order to reduce stress levels.

Some additional units (15 to 50 MW rated power) were analyzed during the RLZ operation to compare the vibrational behavior. The main focus was on the analysis of dynamic instabilities and potentially dangerous consequences of RLZ operation. The goal was to present criteria for allowable (temporary) operation in the RLZ and to determine the relationship between the vortex and the machine vibrations.

Key words: Rough Load Zone (RLZ), vortex, draft tube, pressure pulsation, dynamic loads, axial loads

1 INTRODUCTION

It is well known in practice that machines driven by Francis turbines experience instability in operation on partial loading, typically from 30-50% of load (sometimes even up to 70%), known as Rough Load Zone (RLZ). The source of information for this paper is based on 25 years of experience in machine design, machine operation and maintenance as well as in on-line measurements, monitoring and diagnostics. The primary case study is a 120 MW, 120 RPM Francis turbine hydro generator with RLZ which resulted in severe consequences to the condition of the machine. The relationship between RLZ and machine vibrations was captured with a machine condition monitoring system. Other hydro generators driven by Francis turbines that had strong RLZ manifestations with similar monitoring systems will be studied for comparison.

2 120 MW HYDRO UNIT ANALYSIS

Machine condition monitoring systems were installed and commissioned on 4 machines with 120 MW rated power Francis turbines. They were umbrella type hydro generator designs with the axial bearing below the generator guide bearing and above the turbine guide bearing; GGB (generator guide bearing), TGB (turbine guide bearing). One machine with extended sensor configuration was selected to better understand the condition, behavior and consequently the root cause of the problem that these machines experienced during operation. The configuration of the system in Figure 1 included the following measurements:

- Machine speed (RPM)
- Relative shaft (radial) vibrations
- Absolute bearing (radial) vibrations
- Axial bearing vibrations
- Turbine cover vibrations in axial direction¹
- Axial rotor displacement²
- Stator feet to concrete foundations expansion (radial)³.
- Radial vibrations on draft tube

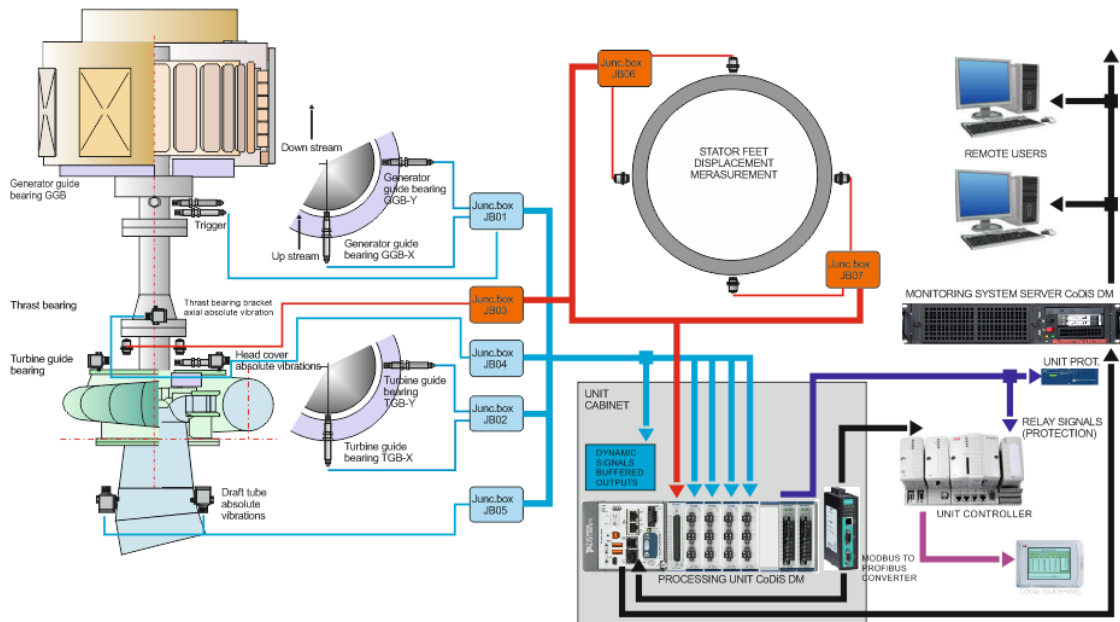


Figure 1 – Monitoring system layout.

Signals from all sensors were simultaneously sampled and processed. All the results were stored to a historical database throughout the machine operational lifetime. The main purpose of installing the monitoring system was to detect, analyze, and fully understand the impact of the RLZ on machine condition. Analysis was conducted through all operating conditions with special attention to the RLZ occurring at ~50 MW load.

3 ANALYSIS OF MONITORING DATA

3.1 Trend data analysis

Vibro-dynamic condition of the unit was based on the vibration trend data compared throughout different machine operating conditions such as:

- Standstill
- Start
- Free run

¹ Two probes at 90°; US = Upstream & RB = Right Bank

² Two probes at 90°; US = Upstream & RB = Right Bank

³ Four probes at 90°; US =Upstream, LB = Left Bank, DS = Downstream & RB = Right Bank

- Synchronized
- Load (incremental)
- Load heated
- Run down with no braking

On-line data analysis included calculating the vector components from the waveform signals in real time. For shaft vibrations this included order analysis (S1n, S2n, S3n amplitude and phase)⁴, Peak, Smax⁵ values, and others. For bearing vibrations this included order analysis RMS, RMS in specific frequency band, Eq Peak, and others for vibration velocity (mm/s RMS).

Figure 2 shows the Smax trend data in two radial bearing planes (GGB and TGB) alongside operating condition indicators recorded during same period. In the zone of 50 MW operation the vibration amplitudes were much higher than the amplitudes recorded during full power load. It appears that the machine passed through the RLZ twice 1) during load increase and 2) during the shut-down process. At 50MW, the TGB vibration amplitudes (Smax) reached a maximum at ~300 µm



Figure 2 - Upper diagram: Smax @ GGB & TGB; Lower diagram: RPM, Active Power (P) & Axial Displacement.

Further analysis required a more detailed observation in that particular power span. Figure 3 is zoomed in while the machine passes through RLZ during the load increase process. The parameters shown are:

- Smax on radial bearings (TGB and GGB),
- RMS on axial (thrust) bearing Vrms (vibration velocity),
- Active Power,
- Guide vane opening,
- Axial displacement

Operating conditions are:

- Run up
- Synchronization
- Load increase to 80MW

⁴ S1n – first harmonic; S2n – second harmonic, S3n – third harmonic of rotational speed frequency, A – Amplitude, Ph – Phase

⁵ Smax is the maximum displacement value obtained from two perpendicular probes

as: $S_{max} = \sqrt{X^2 + Y^2}_{max}$

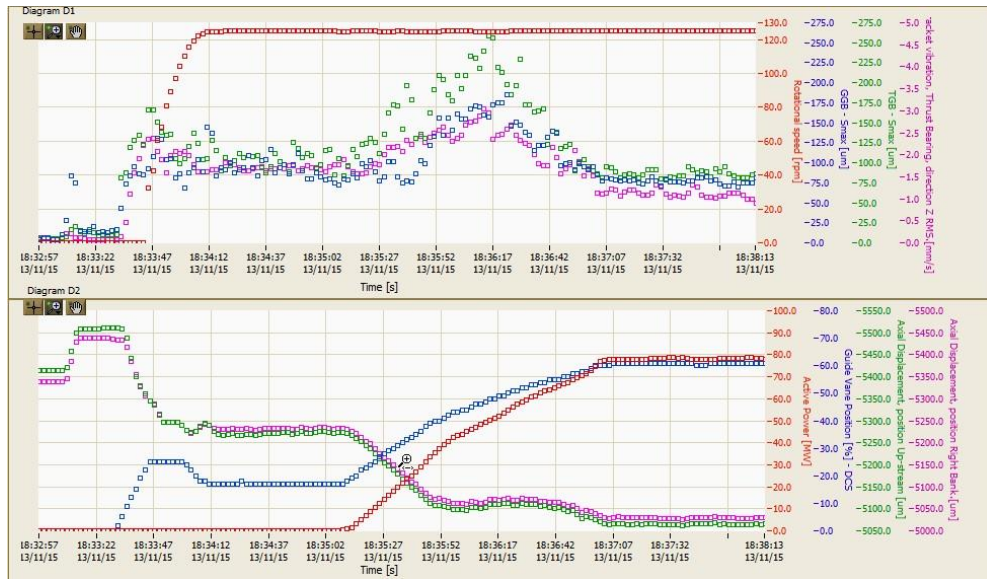


Figure 3 – Upper diagram: *RPM*, *Smax* on *GGB* & *TGB*, *Vrms* on *ThrB* in axial dir; Lower diagram: *P*, *Guide vane opening*, axial displacement *US* (Upstream), and *RB* (Right Bank).

Since RLZ operation can lead to large vibration response in the axial direction it is important to analyze the behavior of axial displacement signals. The axial displacement sensors were located below the rotor so as the rotor moved away from the probe the signal increased. It was visible that during standstill the axial displacements increased by ~100 μm , which was likely an effect caused by the oil lift circulating in the axial bearing. As the machine started to rotate the axial displacement signals decreased as the water pushed down on the rotor. When the machine was in mechanical free run the axial displacement signals were stable.

The axial displacement signals started decreasing with load as more water increased the force acting downwards on the rotor. This was visible during 0 to 40 MW load operation, but more significant results were after 40MW during RLZ operation when the axial displacement increased and achieved a stationary state until the machine reached 60 MW load. After that the axial displacement decreased again as expected, achieving a constant value at a steady load of 80 MW. At the same time, the *Smax* vibration levels on the *TGB* increased from ~80 to 100 μm before the RLZ to over 250 μm at ~50 MW during the RLZ occurrence. Similar behavior with smaller amplitudes were recorded on the *GGB*. Absolute vibrations *Vrms* signal (axial) on the thrust bearing increased up to ~3 mm/s RMS at ~50 MW and then decreased to 0.5 mm/s RMS with load increase.

This led to the conclusion that water energy was being distributed differently during the RLZ occurrence. The momentum on the turbine increased with more water and not due to increased axial force on the turbine rotor. From the vibration amplitude signal components it can be concluded that there was a significant change, however the root cause(s) cannot be found without analyzing the frequency. Order analysis provided amplitudes and phases at certain frequencies related to the machine rotation as well as the Rest⁶ values. Order frequencies can be used to track faults related to machine rotation where the source is from the rotor (e.g. mechanical or electrical unbalance, Run Out⁷, etc...). The Rest value was recorded so the system can detect irregularities on all other frequencies beyond those which are order related.

Figure 4 shows vibration *Smax*, *S1n*, and Rest comparisons with the intention of focusing on specific frequency ranges for further data analysis. *S1n* vibrations did not experience any changes during RLZ, whereas the Rest signal components completely follow the *Smax* behavior and increased during RLZ operation.

⁶ Rest – amplitudes on all frequencies excluding *S1n*, *S2n* and *S3n*

⁷ Slow roll recorded, geometry offset or shaft coupling defect

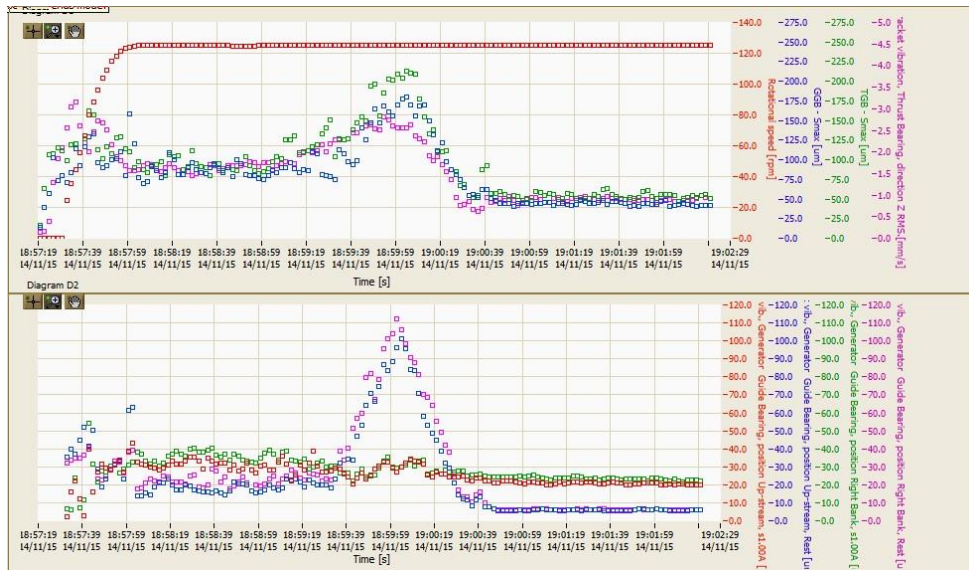


Figure 4 – Upper diagram: RPM, Smax on GGB i TGB, Vrms on ThrB in axial dir; Lower diagram: s1.00A on GGB US and RB, and Rest on GGB US and RB.

Similar behavior can be identified in Figure 5 where the axial vibrations S1n, S2n, Rest, and overall RMS signal of vibration velocity show that the order related amplitudes did not experience any difference during RLZ whereas the Rest signal component increased in the axial bearing vibration.

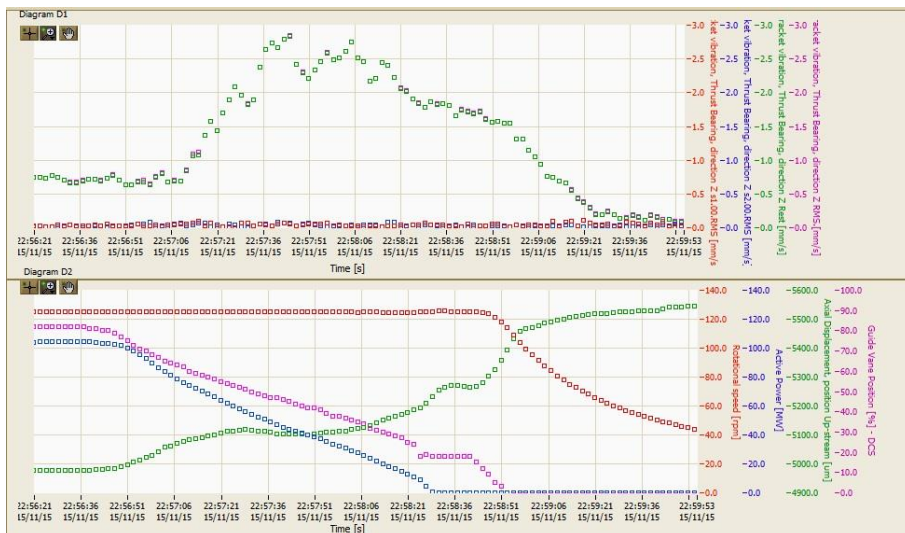


Figure 5 – Upper diagram: Axial (ThrB) – s1.00A and s2.00A, Rest and RMS; Lower diagram: RPM, P, Ax displ US, Guide wane opening.

It should be noted that similar response was present on the Turbine Cover axial vibration but are not presented since Figures 4 and 5 sufficiently describe the machine behavior. It can be concluded that during RLZ operation high vibration amplitudes occurred at specific frequencies not related to the machine rotation. This event represents dynamic instability which requires further analysis in the frequency domain to completely understand the machine behavior, the impact of this instability to the machine, and whether this poses any danger to the reliability of the machine.

3.2. Waveform and Spectrum analysis

The monitoring system recorded both the condition vector⁸ signals (history trend) and raw data which was streamed in case of an event or additional analysis was required. This allowed for post processed analysis using tools such as FFT, as can be seen in Figure 6 with the vibration velocity spectrum

⁸ Condition vector is an array of numbers (scalars and vectors) calculated from signal, in real time, which describes the machine condition. Some of its components are already mentioned such as S1n amplitude and phase.

up to 1000 Hz frequency range. The accelerometers and monitoring system recorded the vibration velocity from 0.5 to 1000 Hz.

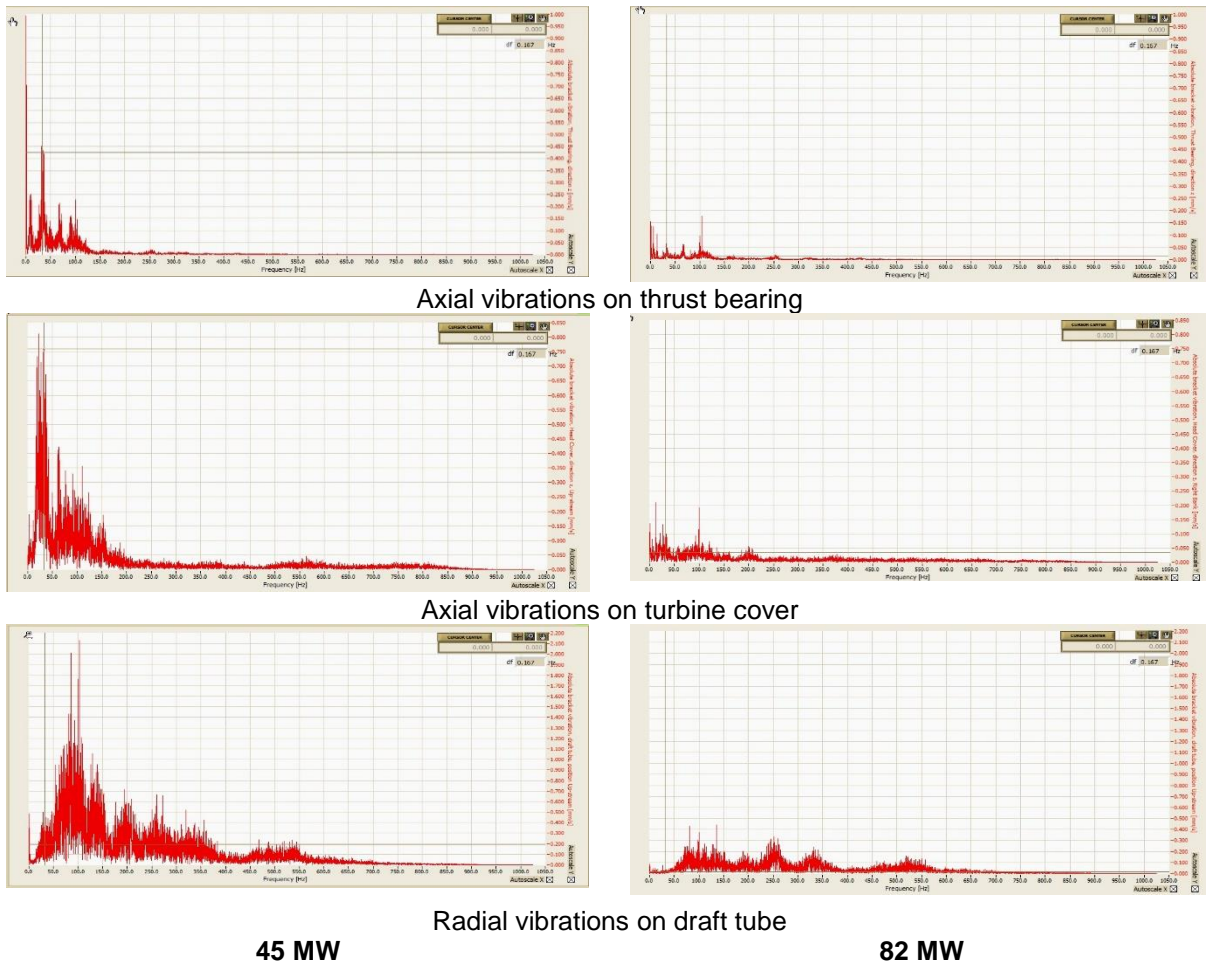


Figure 6 – FFT spectrum diagrams: LEFT SIDE: 45 MW, RIGHT SIDE: 82 MW.

Spectra were recorded during RLZ operation and during steady state operation.

At 45 MW (under RLZ):

- **Draft tube:** There were a lot of frequencies present, up to 600 Hz. This showed that overall RMS was high but evenly distributed mostly between 50 to 100 Hz. A peak at 0.5 Hz was present with lower amplitudes.
- **Turbine cover:** Dominant frequencies were up to ~150 Hz. A peak at 0.5 Hz was present with lower amplitudes.
- **Thrust bearing bracket:** Visible frequencies were up to ~120 Hz but was most dominant at ~0.5 Hz. Since no signal component was visible at other positions, it can be assumed that there was likely resonance in this area of the construction.

At 82 MW (outside RLZ):

- **Draft tube:** Spectrum up to 600 Hz with lower amplitudes at 45 MW which is somewhat typical for hydraulic measurements due to water flow impact on the structure.
- **Turbine cover:** Similar conclusion as for Draft tube
- **Thrust bearing bracket:** there was no 0.5 Hz component outside RLZ.

It can be concluded that on the turbine and draft tube higher vibrations were present due to hydraulic components and water turbulence which were at multiple frequencies as high as 600 Hz. On the Thrust Bearing there were low frequency components present that carry much higher energy and only appeared during RLZ occurrence. To determine the exact behavior more detailed analysis of lower frequencies was required.

Figure 7 shows waveform signals on shaft vibrations at GGB and TGB in the Upstream direction and axial displacement alongside axial vibration velocity and key phasor. The left side shows raw data and vibration velocity (lower diagram, blue signal) and the right side shows a post processed signal through a low pass filter and integrated to displacement. This was recorded during 45 MW load operation.

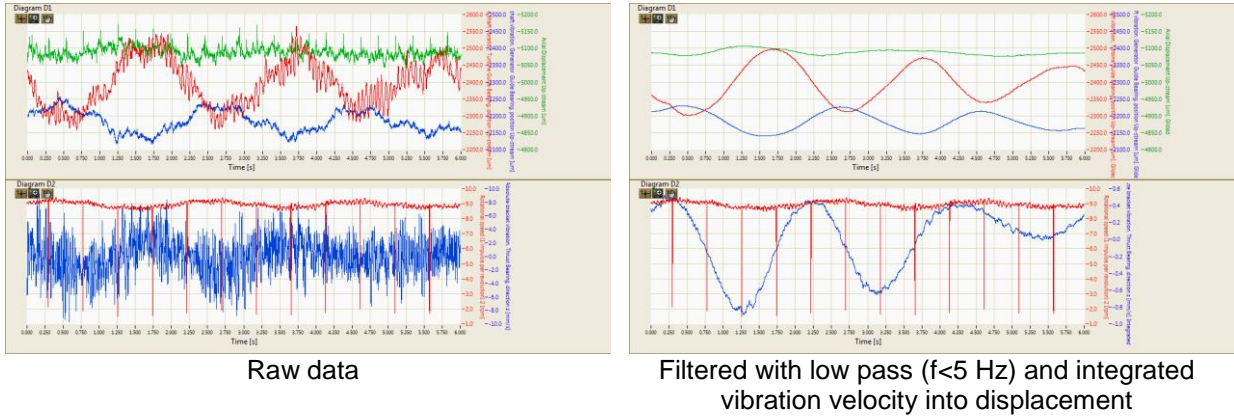


Figure 7 – Raw data on 45 MW. Upper diagram (both left and right): Relative shaft vibrations on TGB – US, GGB – US, Axial displ. – US. Lower diagram: Key phasor i Vibration velocity (left) / Vibration displacement (right) on thrust bearing bracket

All signals were driven by a 0.5 Hz component which is ¼X the rated rotational speed frequency. On the draft tube and turbine cover this frequency component had very low amplitudes (Figure 6) compared to the thrust bearing axial vibrations. The 0.5 Hz component in Figure 7 was not only visible in the axial direction but also in the radial direction of the relative shaft vibration signals. Also, shaft displacements on GGB and TGB were in counterphase which indicates minimal vibration between radial bearings. Rotor axial displacement signals do not show significant amplitudes at 0.5 Hz which means that the rotor was not moving relative to axial bearing bracket at those frequencies. Absolute thrust bearing bracket vibrations (and displacements shown as integrated signal on the right side of Figure 7) showed significant displacement levels at 0.5 Hz frequency. The overall displacement on thrust bearing bracket calculated from the integrated signal was:

$$S_{axl} = 1.3 \text{ mm peak-to-peak}$$

These values are excessive considering the rotor weight and hydraulic downward load was 875 T. The axial displacement of the rotor relative to the bracket was insignificant indicating that the complete rotor including the bearing bracket was vibrating together in the axial direction. Figure 8 shows the sensor position and displacement indication.

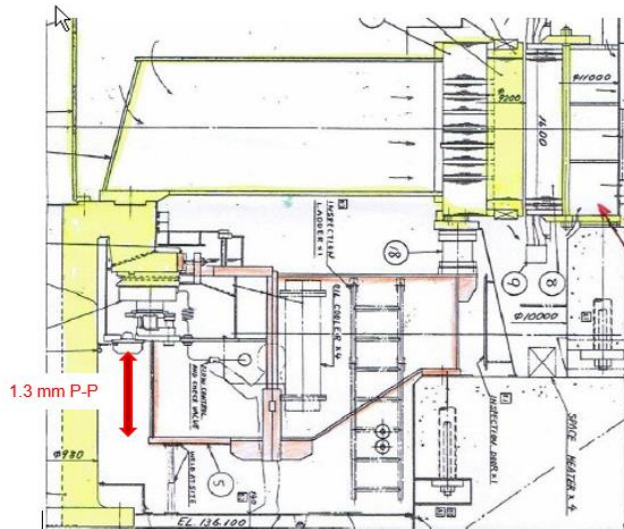


Figure 8 – Generator thrust bearing bracket and measurement point.

These displacement amplitudes generated a lot of stress in the bracket and could threaten the structural integrity. Measurements of axial displacement of the rotor to concrete foundations would be the

best representation of how severe the problem is. These signals could be used to calculate the bracket deformation when excluding the axial displacement of the rotor-to-bracket and bracket-to-foundations.

During RLZ occurrence pressure pulsations under turbine runner could be the result of axial movement of the turbine runner due to large axial displacements. The pulsations may be caused by the rotor instability, so it would be very useful to determine which comes first - the pressure pulsations or the axial (and radial) displacements of the turbine runner and generator rotor. On this unit there were no pressure sensors installed but there were interesting results from other plants that will be described later.

Analyzing the amplitudes and phases of the shaft vibrations indicate that the whole rotor had a precession movement around the rotor mass center as shown in Figure 9. The movement was mostly visible during RLZ occurrence at 45 MW load and practically not present at 82 MW load. To confirm this, an upgraded system with two more axial vibration sensors was recommended. This would allow the phase comparison at all positions and stiffness of the axial bracket to be determined from the response. If the stiffness decreased in any sensor it could be detected and quantified.

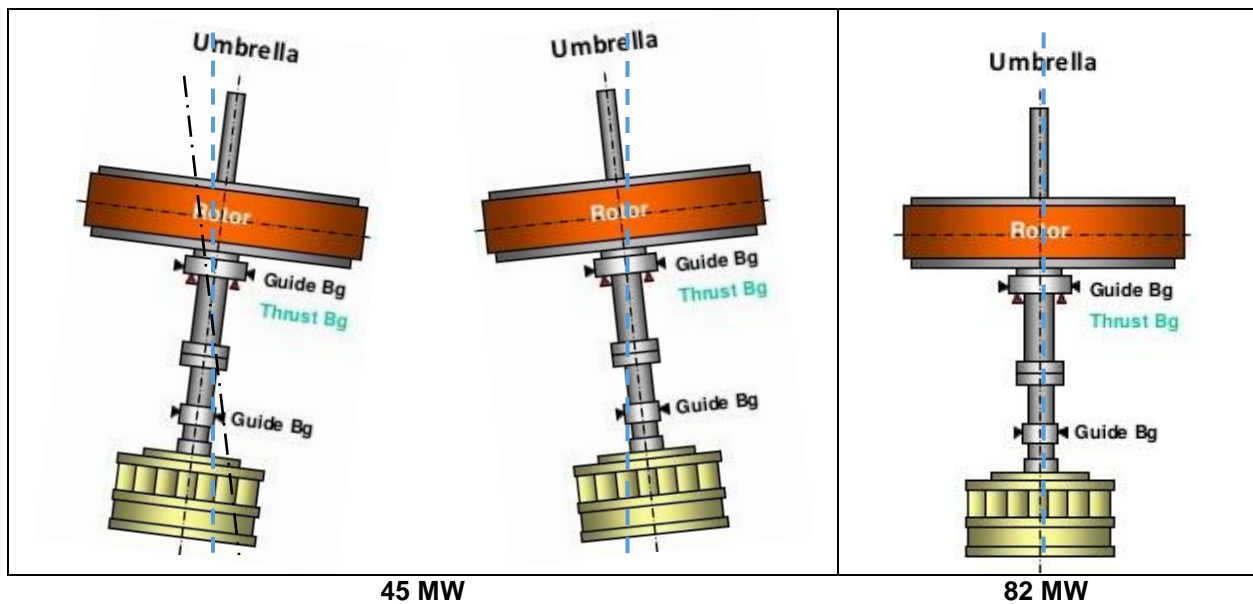
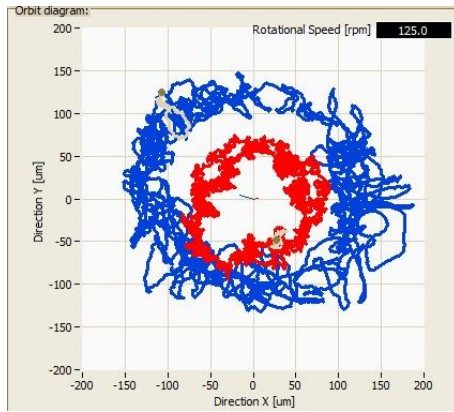
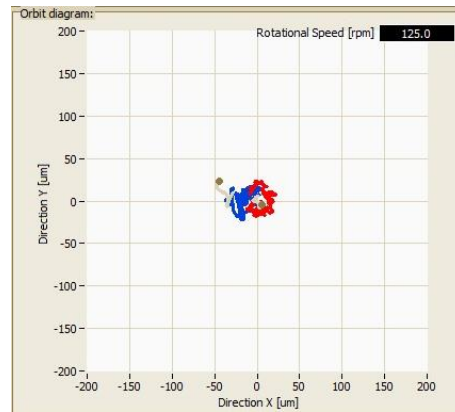


Figure 9 – Rotor precession movement at 0.5 Hz on various loads

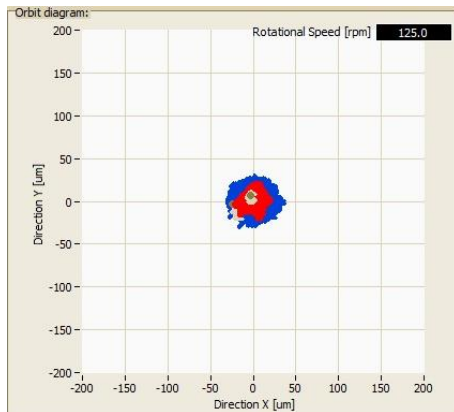
Analysis of the shaft orbits in Figure 10 supports the precession theory. Orbits display the X and Y signal plots from two perpendicular shaft displacement sensors in one bearing plane. Orbits represent the shaft displacement position (both dynamic and steady state) inside the bearing and represent directly the bearing clearance during dynamic operation of the machine. Therefore, they can be an important indicator of how much RLZ affects the bearings. In Figure 10 the orbits recorded during various load operations (50 and 82 MW load) are shown. On the left side, the complete signal duration is shown as X and Y plot from two probes (raw orbits). On the right side, are the orbits averaged per single machine revolution. It appears that low frequency components were affecting the shaft position significantly, but it is not visible from turn to turn. To display the real movement of both the wobbling frequency and the rotational speed simultaneously at least 4 rotations are needed since the wobbling frequency was $\frac{1}{4} \times$ the rotational speed. Comparing the left and right diagrams the low frequency component had significant impact during RLZ occurrence. When the machine operates outside the RLZ (at 82 MW) the wobbling disappeared, and the shaft orbits were at the frequency related to machine speed so both the raw orbit and the averaged orbit were practically the same.



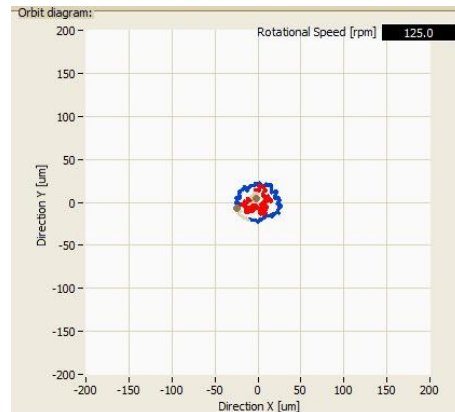
Raw, 50 MW



Averaged per turn, 50 MW



Raw, 82 MW



Averaged per turn, 82 MW

Figure 10 – Orbit diagrams (raw and averaged per turn) on two load conditions (50 MW, and 82 MW), GGB and TGB

The wobbling was present due to the vortex generated under turbine runner, however the response in this case was mostly related to the machine design and the precession movement around the rotor mass which caused large displacements in the radial direction as a result of axial vibrations. The new standard published in 2018 for the measurement and evaluation of vibration in this type of machinery, ISO 20816-5 indicates that shaft orbits (peak-to-peak values of relative shaft vibrations) should not exceed 70% of the cold bearing clearance. In this case the shaft orbits were near this value meaning that there was a significant load on radial bearings in the RLZ. To support this conclusion, cracks have formed in the concrete foundations at the axial bearing thrust bracket supports shown in Figure 11 on another unit of the same design in this power plant that had experienced the same issues while operating in the RLZ.



Figure 11 – Cracks in bearing to foundation supports on other unit in the same plant

4 RESULTS FROM OTHER PLANT

Similar behavior was recorded on a 187.5 RPM, 32 MW umbrella type unit driven by Francis Turbine (faster and smaller than the case described above). The machine experienced RLZ in the load range from 8 to 20 MW at a frequency of ~ 0.8 Hz ($\sim 1/4$ X the rotational speed). The rough load zone effect was not as severe as the above case, but still influenced the machine operation. Three very important data records and analysis findings were made:

1. Mapping the rough load zone throughout a longer period and plotting the head versus power diagram for RLZ.
2. Pressure pulsations recorded alongside other signals provided a new perspective on this phenomenon which will be described.
3. Air was blown under the turbine to eliminate the vortex and the results will be shown.

Data collection was carried out for over one year of operation and provided the possibility to correlate operating conditions with RLZ occurrence and map a machine availability chart dependent on water levels and power shown in Figure 12.

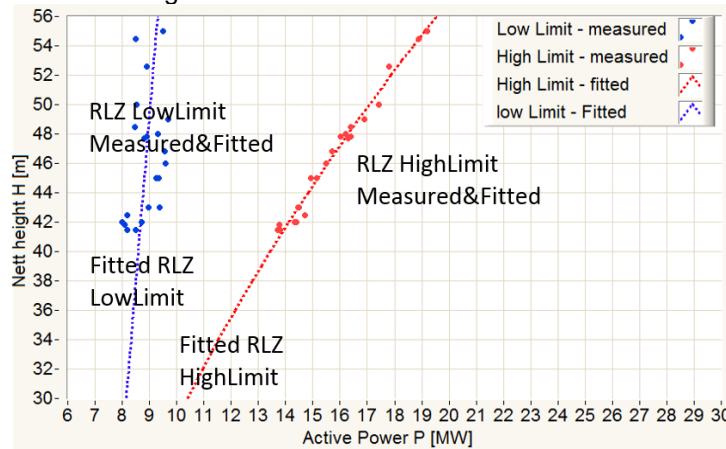


Figure 12 – RLZ mapping chart (Head vs Power)

Another interesting result were the raw waveform data analysis during one of the RLZ events on this machine shown in Figure 13.

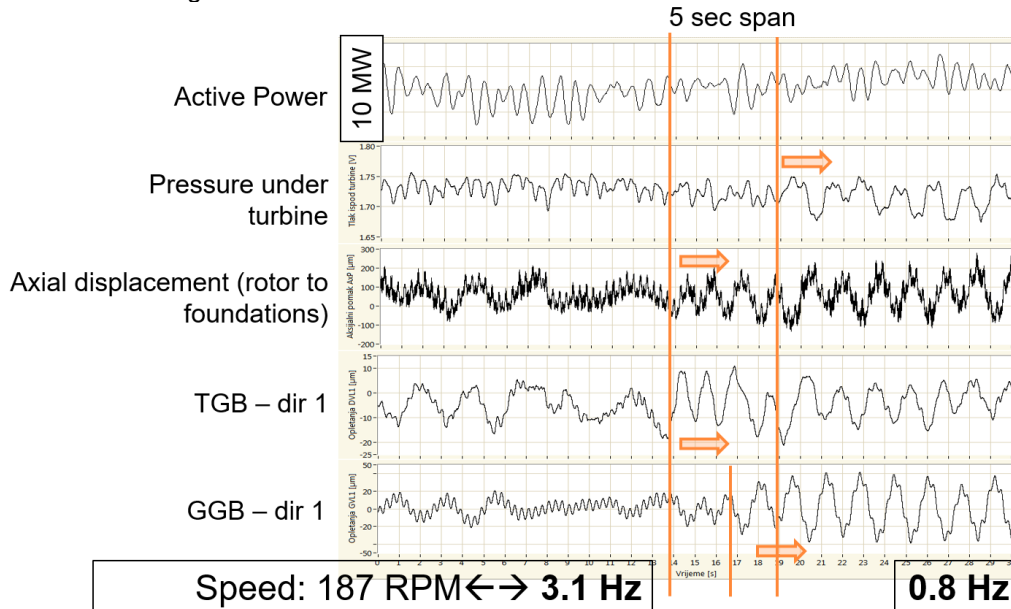


Figure 13 – Raw data recorded during RLZ operation on 10 MW

This 30 second data record represents the start of a vortex and the low frequency wobbling/pulsations at 0.8 Hz. Active power was 10 MW, showing approximately 1 MW fluctuations at 1.2 Hz throughout the complete data record. The most interesting result was the pressure pulsation signal

fluctuation. The pressure started to fluctuate at 0.8 Hz about 5 seconds after the rotor axial displacement and the shaft radial displacements on turbine bearing. The radial displacement on the generator bearing followed the axial and turbine displacement which started at the same time. Pressure pulsations at 0.8 Hz started 5 seconds later. These results were different than expected, as previous experience indicated that the pressure caused the rotor movement. It seems that these results show the opposite and that the axial rotor movement caused the pressure pulsations under turbine runner. Self-excited vibrations may be the cause of this phenomenon due to inadequate energy transformation on the turbine. In RLZ operation water flow on the turbine blades can lose its stability and the turbine does not effectively transfer the water kinetic energy to momentum. The left-over energy must be converted which triggers self-excited vibrations resulting in dynamic instability of machine.

Since RLZ phenomena is related to turbine design and manufacturing there is little that can be done to remove it once present. It can however be mitigated with air admission under the turbine to eliminate the vortex and reduce the vibrations. Data was recorded during that experiment to observe the effect of the air admission on pulsations. Figure 14 shows the shaft displacement amplitude with air blown intermittently into the vortex to test the vortex elimination. The vibrations decreased during the air admission and increased when air was not present.

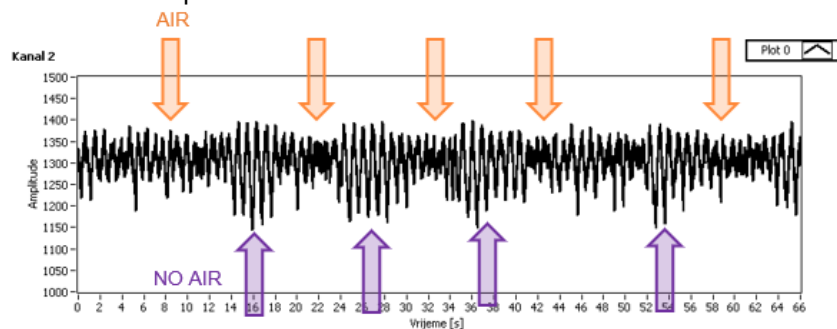


Figure 14 - Shaft displacement waveform at 8 MW - experimenting with air under turbine

There are several available solutions to control the vortex such as fins in the draft tube to decrease the swirl and broaden the operating range, but these are often found to significantly reduce the efficiency. As well, modifications to the turbine cone including extension and/or grooves can be made which do not affect the efficiency as much but the pressure pulsations may cause large forces on the modified cone. The most common solution and the chosen option for this case was air admission directly under the turbine runner, as shown in Figure 15. Where the pressure under the turbine is higher than atmospheric pressure other methods such as “Jet Pump Turbine Air Admission” made by Fuji should be used to overcome the pressure differential.

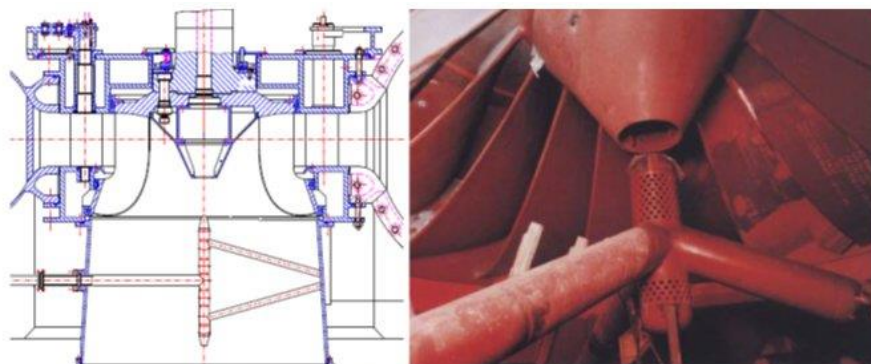


Figure 15 - Air admission directly under the turbine

5 CONCLUSION

Dynamic instabilities on partial load in Francis turbines is well known and there are several studies describing the phenomena. This paper presents a practical insight into how to monitor such phenomena and diagnose the impact on machine condition. Not every machine will react the same and there is no general method to minimize the RLZ affecting the machine operations.

On the 120 MW machine case study the RLZ effect was posing a threat to the machine condition and reduced machine operability/availability. Cracks in the axial bracket to foundation support were found on a sister unit in the same plant. It was found that bracket deflections reached 2 mm peak-to-peak at 0.5 Hz. There was considerable stress in the thrust bracket which led to significant stiffness reduction and machine operability problems. Also, during RLZ occurrence the radial vibrations increased significantly, reaching values of bearing clearance limits as recommended by ISO 20816-5.

The other case study showed that the RLZ was not fixed and very much dependent on upper and lower water levels (head). The power span in which one might expect the instability was changing according to water levels and so too the machine availability. For automated operations where the machines are driven by a dispatch center, this becomes very important information. Therefore, this paper presents the recommendation to map the RLZ for each machine and use that as a guideline for operating the machine remotely.

This paper also briefly considers several methods of reducing the effect of instability which are referenced below for a detailed description. Using the air admission under the turbine can collapse the vortex and effectively reduce the vibrations. Feedback between the monitoring system and the air admission system should be established for this system to work effectively.

6 REFERENCES

- [1] L. A. Vladislavlev, „Vibration of Hydro Units in Hydroelectric Power Plants“, Publikacija, Amerind Publishing Co. Pvt. Ltd, New Delhi, 1979.
- [2] ISO 7919-5:2005, "Mechanical vibration of non-reciprocating machines – Measurements on rotating shafts and evaluation criteria – Part 5: Machines sets in hydraulic power generating and pumping plants", ISO, 2005
- [3] ISO 20816-5:2018, "Mechanical vibration -- Measurement and evaluation of machine vibration -- Part 5: Machine sets in hydraulic power generating and pump-storage plants"
- [4] M. Jadrić, B. Rajković, B. Terzić, V. Firinger, M. Despalatović, Ž. Gladina, G. Orešković, B. Meško, J. Macan: "NADZOR HIDROAGREGATA - Stanje i razvoj u Hrvatskoj elektroprivredi, proizvodno područje HE Jug", Studija
- [5] G. Orešković, T. Tonković, O. Husnjak, Technical report TR25112015, VESKI, Zagreb, RH, November 2015
- [6] CEATI report No T082700-0364, "Hydraulic phenomena that occur in operating hydraulic turbines", March 2011
- [7] Foroutan, Hosein & Yavuzkurt, Savas. (2014). Flow in the Simplified Draft Tube of a Francis Turbine Operating at Partial Load—Part II: Control of the Vortex Rope. *Journal of Applied Mechanics*. 81. 10.1115/1.4026818.
- [8] Nishi, M., Wang, X. M., Yoshida, K., Takahashi, T., and Tsukamoto, T., 1996, "An Experimental Study on Fins, Their Role in Control of the Draft Tube Surging," *Hydraulic Machinery and Cavitation*, E. Cabrera, V. Espert, and F. Martinez, eds., Kluwer Academic Publishers, Dordrecht, Netherlands, pp. 905–914.
- [9] Falvey, H. T., 1971, "Draft Tube Surges—A Review of Present Knowledge and an Annotated Bibliography," U.S. Department of the Interior, Bureau of Reclamation, Report No. REC-ERC-71-42.
- [10] Vevke, T., 2004, "An Experimental Investigation of Draft Tube Flow," Ph.D. thesis, Norwegian University of Science and Technology, Trondheim, Norway.
- [11] Sanol, T., Maekawa, M., Okamoto, N., Yano, H., and Miyagawa, K., 2012, "Investigation of Flow Pattern Downstream of Spiral Grooved Runner Cone in Pump-Turbine," 26th IAHR Symposium on Hydraulic Machinery and Systems, Beijing, China, August 19–23.
- [12] Qian, Z. D., Li, W., Huai, W. X., and Wu, Y. L., 2012, "The Effect of the Runner Cone Design on Pressure Oscillation Characteristics in a Francis Hydraulic Turbine," *Proc. IMechE A J. Power Energy*, 226(1), pp. 137–150.
- [13] Papillon, B., Sabourin, M., Couston, M., and Deschenes, C., 2002, "Methods for Air Admission in Hydro Turbines," 21st IAHR Symposium on Hydraulic Machinery and Systems, Lausanne, Switzerland, September 9–12.